eNeuro

Research Article: New Research | Development

Morphological and phagocytic profile of microglia in the developing rat cerebellum

Microglia in the developing cerebellum.

Miguel Perez-Pouchoulen[1], Jonathan W. VanRyzin[1,2] and Margaret M. McCarthy[1,2]

[1]*Department of Pharmacology, University of Maryland School of Medicine, Baltimore, MD, USA 21201*
[2]*Program in Neuroscience, University of Maryland School of Medicine, Baltimore, MD, USA 21201*

DOI: 10.1523/ENEURO.0036-15.2015

Received: 21 April 2015

Revised: 8 August 2015

Accepted: 12 August 2015

Published: 18 August 2015

Author Contributions: M.P.P. and M.M.M. designed research; M.P.P. performed research; J.W.V. and M.M.M. contributed unpublished reagents/analytic tools; M.P.P. analyzed data; M.P.P. and M.M.M. wrote the paper.

Funding: National Institute of Health: R01-MH091424. Consejo Nacional de Ciencia y Tecnologia: 236296.

Conflict of Interest: The authors declare no competing financial interests.

Correspondence should be addressed to Dr. Miguel Perez-Pouchoulen, 655 W. Baltimore Street, BRB-5-014, Baltimore, MD 21201. Tel: 4104062654. Email: mpouchoulen@som.umaryland.edu

Cite as: eNeuro 2015; 10.1523/ENEURO.0036-15.2015

eNeuro

http://eneuro.msubmit.net

eN-NWR-0036-15R3

Morphological and phagocytic profile of microglia in the developing rat cerebellum

Manuscript Title Page

1. Manuscript Title

Morphological and phagocytic profile of microglia in the developing rat cerebellum.

2. Abbreviated Title

Microglia in the developing cerebellum.

3. List all author Names and Affiliations

Miguel Perez-Pouchoulen[1], Jonathan W. VanRyzin[1,2], Margaret M. McCarthy[1,2]

[1]Department of Pharmacology and [2]Program in Neuroscience, University of Maryland School of Medicine, Baltimore, MD, USA 21201.

4. Author Contributions

M.P.P. and M.M.M. designed research; M.P.P. performed research; J.W.V. and M.M.M. contributed unpublished reagents/analytic tools; M.P.P. analyzed data; M.P.P. and M.M.M. wrote the paper.

5. Correspondence should be addressed to

Dr. Miguel Perez-Pouchoulen and Dr. Margaret M. McCarthy.

655 W. Baltimore Street, BRB-5-014, Baltimore, MD 21201

email: mpouchoulen@som.umaryland.edu, jvanryzin@umaryland.edu, mmccarthy@som.umaryland.edu

6. Number of Figures: 7.

7. Number of Tables: 2.

8. Number of Multimedia: none.

9. Number of words for Abstract: 245.

10. Number of words for Significance Statement: 120.

11. Number of words for Introduction: 713.

12. Number of words for Discussion: 1562.

13. Founding sources

This work was supported by the NIH Grant R01-MH091424 to M.M.M. and CONACYT (Consejo Nacional de Ciencia y Tecnologia, Mexico) Postdoctoral Fellowship 236296 to M.P.P.

14. Conflict of Interest

The authors declare no competing financial interests.

15. Acknowledgements

This work was supported by the NIH Grant R01-MH091424 to M.M.M. and CONACYT (Consejo Nacional de Ciencia y Tecnologia, Mexico) Postdoctoral Fellowship 236296 to M.P.P.

Abstract

Microglia are being increasingly recognized as playing important roles in neurodevelopment. The cerebellum matures postnatally, undergoing major growth, but the role of microglia in the developing cerebellum is not well understood. Using the laboratory rat we quantified and morphologically categorized microglia throughout the vermis and across development using a design-based unbiased stereology method. We found that microglial morphology changed from amoeboid to ramified during the first three postnatal weeks in a region specific manner. These morphological changes were accompanied by the sudden appearance of phagocytic cups during the third postnatal week from PN17 to PN19, with a >4-fold increase compared to the first week, followed by a prompt decline at the end of the third week. The microglial phagocytic cups were significantly higher in the granular layer (~69 %) than in the molecular layer (~31 %; ML) during a three-day window, and present on ~67 % of microglia with thick processes and ~33 % of microglia with thin processes. Similar proportions of phagocytic cups associated to microglia with either thick or thin processes were found in the ML. We observed cell nuclei fragmentation and cleaved caspase-3 expression within some microglial phagocytic cups, presumably from dying granule neurons. At PN17 males showed a ~ 2-fold increase in microglia with thin processes compared to females. Our findings indicate a continuous process of microglial maturation and a non-uniform distribution of microglia in the cerebellar cortex that implicates microglia as an important cellular component of the developing cerebellum.

Significance statement

Microglia are the resident immune cells of the brain and constantly survey their local environment in order to eliminate cellular debris after injury or infection. During brain development, microglia participate in neurite growth, synaptic pruning, and apoptosis, all of which are essential processes to the establishment of neuronal circuits. The cerebellum undergoes major growth and synaptic reorganization after birth, leading to the development of cerebellar circuits which are involved in motor

and cognitive functions. The role of microglia in the developing cerebellum is not well understood. This study provides important foundational profiles of microglial development in the cerebellum, a vulnerable structure to alteration during development, and contributes to the growing appreciation of the clearance activity of microglia during postnatal development.

Introduction

Microglia are the resident macrophages of the central nervous system (CNS) and play important roles during both normal functioning and in disease or injury. Microglia exhibit diverse morphological features across the CNS and phases of the lifespan (Tremblay et al., 2011). In the adult brain, microglia are known to actively survey their environment through their ramified processes and they dramatically change their morphology in response to damage or infection in order to repair the CNS (Ayoub and Salm, 2003; Nimmerjahn et al., 2005; Ransohoff and Perry, 2009; Nayak et al., 2014). These morphological changes are accompanied by phagocytosis to remove dead cells or cellular debris (Vargas et al., 2005; Catalin et al., 2013), giving microglia the title of the scavengers of the CNS. Recent evidence suggests microglia are involved in normal development of the brain including neurite growth, synaptic pruning, spinogenesis and apoptosis (Marin-Teva et al., 2004; Paolicelli et al., 2011; Schafer et al., 2012; Lenz et al., 2013; Kaur et al., 2014). During development microglia undergo morphological changes in both cell body and configuration of their processes, changing from round to ramified, with intermediate stages as the brain matures (Wu et al., 1992; Schwarz et al., 2012). Thus, microglia have important functions impacting the development and formation of neural circuits in the CNS. What is not well understood is whether these functions occur according to a developmental timeframe and how they might differ between brain regions.

The cerebellum is a brain structure involved in many functions including motor control and coordination (Glickstein, 1992; Glickstein et al., 2009), as well as non-motor functions such as

attention, working memory, language, nociception, pain, addiction, and reward (Rapoport et al., 2000; Gottwald et al., 2003; Holstege et al., 2003; Saab and Willis, 2003; Miquel et al., 2009; Strick et al., 2009; Durisko and Fiez, 2010; Moulton et al., 2010; Murdoch, 2010; Moulton et al., 2014; Strata, 2015). The anatomy of the cerebellum consists of an organized and uniform cytoarchitecture that allows systematic and efficient communication among the cerebellar neurons (Voogd and Glickstein, 1998; Sillitoe and Joyner, 2007; Apps and Hawkes, 2009). The human cerebellum matures postnatally and undergoes major growth and neuronal reorganization during the first two years after birth (Abraham et al., 2001; ten Donkelaar et al., 2003; Butts et al., 2014). In rats, cerebellar maturation occurs during the first three postnatal weeks with dramatic anatomical changes involving an increase in both cell density and mass volume (Heinsen, 1977; Altman, 1982; Goldowitz and Hamre, 1998). The cerebellar cortex consists of three anatomical layers containing different types of neurons with distinct timeframes of maturation. Maturation of the cerebellar circuitry involves the production and removal of cells as well as spinogenesis and synaptogenesis, among others (Altman, 1972; Wood et al., 1993; Sarna and Hawkes, 2003; Tanaka, 2009; Haraguchi et al., 2012). Microglia regulate synapses in the developing brain in areas such as the visual cortex, hippocampus and retinogeniculate system (Tremblay et al., 2010; Paolicelli et al., 2011; Schafer et al., 2012). However, the number of studies on the role of microglia during postnatal development remain relatively low. In the cerebellum microglia are distributed in both grey and white matter throughout the lifespan across diverse species, and there is a distinct arrangement of microglia processes according to location in the cerebellar cortex (Ashwell, 1990; Vela et al., 1995; Cuadros et al., 1997). Microglia can induce apoptosis of Purkinje neurons *in vitro* (Marin-Teva et al., 2004) but this is not established *in vivo* under normal conditions and overall the role of microglia during postnatal development of the cerebellum is not well understood.

The overarching goal of this report is to profile anatomical changes of microglia during postnatal development of the cerebellum. We hypothesized microglia change their morphological

profile and cell density in direct relationship to the maturation of the cerebellum as well as the anatomical location within the cerebellar cortex. Thus, the purpose of the current study was two-fold: first, to identify the morphological profile of microglia across the postnatal developing cerebellum using the ionized calcium-binding adapter molecule 1 (Iba1), which is a microglia marker (Ito et al., 1998); and second, to determine whether the morphological profile of microglia as well as their phagocytic capability differ according to location in the cerebellar cortex.

Materials & Methods

Animals

Timed pregnant Sprague-Dawley rats purchased from Charles River or raised in our breeding colony were allowed to deliver naturally under standard laboratory conditions. Male and female rat pups were used and the day of birth was denoted as postnatal day 0 (PN0). All animals were housed in polycarbonate cages (20 x 40 x 20 cm) with corncob bedding under 12:12 h reverse light/dark cycle, with *ad libitum* water and food. All animal procedures were performed in accordance with the University of Maryland animal care and use committee's regulations.

Immunohistochemistry

Animals were deeply anesthetized with Fatal Plus (Vortech Pharmaceuticals) and transcardially perfused with 0.9 % saline solution followed by 4 % paraformaldehyde. The entire cerebellums were removed and postfixed overnight in 4 % paraformaldehyde, and cryoprotected with 30 % sucrose until they were saturated. The cerebellums were sagittally sectioned on a cryostat at a thickness of 45 µm. Free-floating cerebellar slices from different time points between PN5 and PN21 were rinsed with 0.1 M phosphate buffered saline (PBS), incubated with 3 % hydrogen peroxide in PBS for 30 min, and then rinsed again. Sections were co-incubated with a polyclonal antibody against Iba1 (1:10000, Wako Chemicals USA, Inc.), a microglia marker (Ito et al., 1998), in 10 % of bovine serum albumin (BSA) in

PBS with 0.4 % Triton X-100 (PBS-T) for 30 min at room temperature (RT) with constant agitation, then kept for 24 h at 4 °C with constant agitation. Subsequently, sections were rinsed in PBS and incubated with biotinylated anti-rabbit secondary (1:500, Vector Laboratories, Inc.) in 0.4 % PBS-T for 1 h at RT followed by rinses in PBS. Sections were incubated with ABC complex (1:500, Vector Laboratories, Inc.) in 0.4 % PBS-T for 1 h at RT. Iba1 positive-cells were visualized using nickel-enhanced diaminobenzidine (Sigma D-5905) as chromogen for 8-10 min incubation at which point sections displayed a dark purple staining. Finally, sections were exhaustively rinsed in PBS, mounted on silane-coated slides, cleared with ascending alcohol concentrations, defatted with xylene, and coverslipped with DPX mounting medium.

Fluorescence immunohistochemistry

In order to co-localize microglial phagocytic cups and fragmented nuclei, Iba1 and DAPI were used, respectively. Free-floating tissue sections from PN17 cerebellums were rinsed with 0.1 M PBS, incubated with 3% hydrogen peroxide in PBS for 30 min, rinsed and then incubated with 0.3 M glycine in 0.4% PBS-T for 60 min. Subsequently, sections were incubated with Iba1 (1:1000, Wako Chemicals USA, Inc.) in 0.4 % PBS-T containing 10% BSA for 30 min at RT with constant agitation and then kept for 24 h at 4 °C with constant agitation. After primary incubation, sections were rinsed in PBS and incubated with the secondary antibody anti-rabbit Alexa Fluor® 594 (1:500; Invitrogen) in PBS-T for 120 min in the dark. Sections were then rinsed, mounted and cover- slipped using Hardset mounting medium containing DAPI (Vector Laboratories, Inc.).

In order to co-localize dead or dying cells with microglial phagocytic cups, we followed the fluorescence protocol described above to identify the cellular death marker cleaved caspase-3 (1:750, Cell Signaling Technology) and Iba1 (1:1000, Abcam) on PN17 cerebellar sections (both cleaved caspase-3 and Iba1 antibodies were incubated together). Anti-rabbit Alexa Fluor® 488 (1:500; Invitrogen) and anti-goat Alexa Fluor 594® (1:500, Invitrogen) were used as secondary antibodies.

Nissl staining

Sagittal sections (45 µm) from PN5, PN7, PN14, PN17 and PN21 vermis were stained with cresyl violet in order to identify pyknotic bodies. Cerebellar sections were washed with PBS 0.1 M, mounted and dried for 24 h. Subsequently, sections were hydrated with a series of decreasing concentrations of ethanol (95 %, 70 % and 50%) for 2 min followed by two washes of distilled water (dH_2O) for 1 min. After a 30 sec incubation in 0.1 % cresyl violet, sections were washed with dH_2O for 1 min and, then incubated in 70 % ethanol for 2 min before the differentiation step in 5 % alcohol acid (95 % ethanol + 5 % acetic acid) for 5 min. Sections were then dehydrated with 2 washes of 95 % ethanol for 2 and 1 min, respectively, and a final incubation in Xylene for 3 min before cover slipping with DPX.

Stereological counts

A design-based unbiased stereological method was performed to quantify microglia, phagocytic cups and pyknotic bodies across the mid-vermis. We used StereoInvestigator 10 software (Microbrightfield) interfaced with a Nikon Eclipse 80i microscope and an MBF Bioscience 01-MBF-2000R-F-CLR-12 Digital Camera (Color 12 BIT). Six counting regions (cerebellar lobules 1, 3, 5, 6, 8, and 10; Figure 1A) from every cerebellar section were used for analysis, which are representative of the anterior, posterior, dorsal and ventral regions of the vermis. A total of 4 cerebellar sections per animal were used with a physical distance of 225 µm between them. Considering the small size of microglial cells, it is unlikely that any cell was counted twice during the stereological analysis. The optical fractionator probe method was used to estimate cell, phagocytic cup and pyknotic body densities using a 100 µm x 100 µm counting frame sampling every 200 µm. We set an optical dissector height of 15 µm with a 2 µm guard zone (top and bottom) to account any change in section thickness during the staining procedure. Both $Iba1^+$ cells and phagocytic cups were counted at 20x magnification, and pyknotic bodies counts and the diameter of phagocytic cups at 40x magnification. All quantifications were carried out under blinded experimental conditions. The overall estimated volume of each counting

194 region sampled in the vermis was used to normalize estimated counts in order to obtain an estimation
195 of the average density of objects of interest (e.g., microglia, phagocytic cups, pyknotic bodies), which
196 was expressed as an estimated number/µm³ (relative density measurement). Although perivascular
197 macrophages are also positive for Iba1, they represent approximately 4 % of the $Iba1^{+}$ population in the
198 brain (Williamson et al., 2011), suggesting a negligible impact of this factor on the data analysis.

199 **Developmental profile of microglia and phagocytic cups**

200 Microglia counts were performed on PN5, PN7, PN10, PN12, PN14, PN17 and PN21 cerebellums
201 from intact male and female rat pups (n = 4, 2 males + 2 females for each group). Microglia were
202 morphologically characterized based on Lenz et al. (2013) with modifications into 4 categories; 1)
203 round/amoeboid microglia, 2) stout microglia, 3) microglia with thick processes (short or long) and 4)
204 microglia with thin processes (short or long), as also described by others (Wu et al., 1992; Gomez-
205 Gonzalez and Escobar, 2010; Schwarz et al., 2012). For descriptive purposes we identified microglia
206 with thick and thin processes as follows: microglia with thick processes are large cells with an
207 amorphous cell body and with at least 2 ramified short, long or both thick processes. Microglia with
208 thin processes are large or small cells with a round and small cell body, with at least 4 ramified short,
209 long or both thin processes (more ramified than microglia with thick processes). The density of total
210 microglia, i.e., regardless of morphology, was obtained by summing all 4 microglial morphologies
211 described above. In addition, cup-shaped invaginations of the plasma membrane formed around cellular
212 debris, infectious agents or dead cells, and called “phagocytic cups” (Swanson, 2008) were also
213 counted in the same cerebellar sections stained with Iba1. In order to have a clear identification of
214 phagocytic cups, only those located at the tip of microglia processes with a round morphology were
215 counted (see Figure 3B-C). All counts were performed solely in the cerebellar cortex; the white matter
216 was not included. Cellular layers (granular versus molecular) were not distinguished in this experiment,
217 as they are not fully formed at the younger ages.

Quantification of microglia and phagocytic cups in the GL and ML

In a separate cohort of animals, microglia and phagocytic cup counts were performed in the granular (GL) and the molecular layer (ML) of the cerebellar cortex on PN12, PN14, PN17 and PN21 male and female rat pups (n = 6, 3 males + 3 females for each group). At these ages both the GL and ML are well developed. Microglia were categorized based on their morphological features as described above and the density of total microglia was also obtained.

Quantification of phagocytic cups during the third postnatal week of development

In a third animal cohort aged PN15, PN16, PN17, PN18 and PN19 (n = 3 males + 3 females for each group) the phagocytic cups were counted in both the GL and ML. The morphology of microglia associated with the phagocytic cups was also quantified.

Quantification of pyknotic bodies

Pyknotic bodies were identified using the cresyl violet staining method on *PN5, ^PN7, *PN14, *PN17 and *PN21 (*n = 6, 3 males + 3 females; ^n = 4, 2 males + 2 females). Pyknotic cell quantification was performed using sections from the cerebellar tissues used in the "developmental profile of microglia and phagocytic cups" experiment and followed the same stereological parameters as described above. Likewise, stereological counting was performed in both the GL and ML of the cerebellar cortex.

Phagocytic cup size

The size of microglia phagocytic cups located in both the GL and ML were measured using the quick circle tool on StereoInvestigator 10 (same microscope and camera specifications described above). The same cerebellar regions (cerebellar lobules) used for stereological counts and 4 cerebellar slices previously stained for Iba1 from ^PN10, *PN14, *PN17 and *PN21 cerebellums (^n = 4, 2 males + 2

239 females; *n = 8, 4 males + 4 females) were used in this assay. This analysis was performed on 16
240 phagocytic cups per animal, which was the averaged for a single measure per animal.

241 **Statistical analysis**

242 All data are expressed as mean ± S.E.M. and effect size estimate calculations (η and d) reported in
243 Table 1 and 2. Developmental profile of microglia and phagocytic cup data sets were analyzed using a
244 one-way ANOVA with age as fixed factor. Data sets from microglia and phagocytic cup counts in the
245 GL and ML, phagocytic cup counts during the third postnatal week of development, nissl staining and
246 pyknotic bodies counts and phagocytic cup size measurement were analyzed using a two-way ANOVA
247 with age and cerebellar layer as fixed factors. All statistical analysis followed a *post hoc* pairwise
248 comparison using the Holm's sequential Bonferroni correction to control for familywise error. Sex
249 differences were studied in the microglia and phagocytic cup counts in the GL and ML data set only at
250 PN17 using a Student's t-test for each dependent variable. A summary of statistical analysis performed
251 is reported in Table 1 and pairwise comparisons in Table 2. Significance was denoted when $p \leq 0.05$.
252 All statistical tests were computed in SPSS 22 and graphed using GraphPad Prism 6.

253 **Results**

254 **Microglia increase during the first three postnatal weeks of development in an age-specific**
255 **manner.**

256 The density of total microglia significantly increased during postnatal development ($p < 0.000$; Figure
257 1B)[a]. A significant increase in total microglia, compared to PN5, was found at PN10 ($p = 0.004$), PN17
258 ($p = 0.012$), and PN21 ($p = 0.010$), but not at PN7 ($p = 0.322$), PN12 ($p = 0.249$) or PN14 ($p = 0.125$).
259 In addition, the proportion of microglia found in each morphological category changed as the
260 cerebellum developed postnatally. While the proportion of stout microglia were more predominant

between PN5-PN7, the proportion of microglia with both thick and thin processes were more abundant between PN10-PN14 and PN17-PN21, respectively (Figure 1B).

Amoeboid and stout microglia decrease whereas microglia with both thick and thin processes increase as the cerebellum matures.

We categorized and counted microglia based on their morphological features across the vermis at different time points during postnatal development. The density of amoeboid microglia were the least common and they significantly decreased after the first postnatal week ($p < 0.000$)[b]. Compared to PN5 there were significantly fewer amoeboid microglia at later ages from PN10 to PN21 {PN10; $p = 0.04$, PN12; $p = 0.009$, PN14; $p = 0.007$, PN17; $p = 0.007$, and PN21; $p = 0.007$, except at PN7; $p = 0.232$; Figure 2A}. Likewise, the density of stout microglia decreased after the first postnatal week ($p < 0.000$)[c] from PN12 to PN21 compared to PN5 {PN12; $p = 0.001$, PN14; $p < 0.000$, PN17; $p < 0.000$, and PN21; $p < 0.000$}, but not at PN7 ($p = 0.706$) or PN10 ($p = 0.108$; Figure 2B). In contrast, the density of microglia with thick processes significantly increased after the first week ($p < 0.000$)[d] with there being more on PN7 ($p = 0.038$), PN10 ($p < 0.000$), PN12 ($p < 0.000$) and PN14 ($p = 0.002$) compared to PN5. However, by the third postnatal week (*PN17 and ^PN21) the density of thick processed microglia dropped back down to immature levels (*$p = 0.102$ and ^$p = 0.167$, respectively; Figure 2C). By contrast, the density of microglia with thin processes steadily increased as the cerebellum developed ($p < 0.000$)[e] with a significant difference from PN10 until PN21 {PN10; $p = 0.002$, PN12; $p = 0.015$, PN14; $p = 0.003$, PN17; $p < 0.000$, PN21; $p < 0.000$ compared to PN5; Figure 2D}.

The density of microglia phagocytic cups peaks during the third postnatal week of cerebellar development.

The frequency of phagocytic cups changed across development ($p < 0.000$)[f], with the highest density observed on PN17 when compared to each time point in this experiment (PN5; $p < 0.000$, PN7; $p < 0.000$, PN10; $p < 0.000$, PN12; $p < 0.000$, PN14; $p < 0.000$, PN21; $p < 0.000$; Figure 3A).

There are more microglia in the granular layer than the molecular layer in the cerebellar cortex.

To test whether the density of total microglia and/or their morphology differs based on anatomical location in the cerebellar cortex, we counted microglia separately in both the GL and ML at different time points during postnatal development. A significant interaction for age X cerebellar layer was found for total microglia ($p < 0.000$)[g]. The GL layer had a higher density of total microglia compared to the ML at PN12 ($p = 0.007$), PN14 ($p = 0.025$), PN17 ($p = 0.010$) and PN21 ($p < 0.000$) (Figure 4A). When we looked at the microglial morphology, there was a significant interaction of age X cerebellar layer for stout microglia ($p = 0.05$)[i]. The ML exhibited a higher density of stout microglia than GL at PN12 ($p < 0.000$), PN17 ($p = 0.007$) and PN21 ($p < 0.000$), but not at PN14 ($p = 0.261$) (Figure 4C). Likewise, a significant interaction for age X cerebellar layer was detected for microglia with thin processes ($p < 0.000$)[k]. We found the GL to have higher density of microglia with thin processes than the ML later in development (PN17; $p = 0.05$, PN21; $p < 0.000$), but not earlier (PN12; $p = 0.56$, PN14; $p = 0.91$; Figure 4E). No significant interactions for age X cerebellar layer were found for round/amoeboid microglia ($p = 0.74$; Figure 4B)[h] or for microglia with thick processes ($p = 0.88$; Figure 4D)[j].

Phagocytic cups are more frequent in the GL than the ML of the vermis during the third postnatal week.

A significant interaction for age X cerebellar layer for phagocytic cups was also found ($p < 0.000$)[l]. Post hoc pairwise comparison revealed a higher density of phagocytic cups in the ML than the GL at younger ages (PN12; $p = 0.002$ and PN14; $p = 0.037$). However, this pattern reversed at slightly older

ages with the GL exhibiting more phagocytic cups than the ML at PN17 ($p < 0.000$,) and PN21 ($p = 0.046$) (Figure 5A).

Because phagocytic cups in the developing cerebellum were highest at PN17 in the GL (Figure 3A and 5A), we sought to determine whether this peak was exclusive to that age or more broadly present. Therefore, we counted phagocytic cups on two consecutive days before and after PN17 in both the ML and the GL of the cerebellar cortex. There was a significant interaction for age X cerebellar layer in phagocytic cups ($p = 0.001$)[m]. Post hoc pairwise comparisons revealed the density of phagocytic cups in the GL was lower at PN15 ($p = 0.003$) and PN16 ($p = 0.05$) compared to PN17 (Figure 5B). No significant differences were found for phagocytic cup density at PN18 ($p = 0.583$) or PN19 ($p = 0.615$) compared to PN17 (Figure 5B), indicating a plateau from PN17 to PN19. In contrast, in the ML the density of phagocytic cups significantly decreased at PN19 compared to PN17 ($p = 0.043$; Figure 5B). Additionally, we replicated the significant difference between the GL and ML in terms of phagocytic cup density. The GL had a greater density of phagocytic cups than the ML from PN16 to PN19 {PN16; $p = 0.012$, PN17; $p = 0.002$, PN18; $p < 0.000$, and PN19; $p = 0.007$, but not at PN15 $p = 0.467$; Figure 5B}.

Additionally, we found the phagocytic cups located in the GL associated exclusively with ramified microglia, with thick and thin processes, from PN15 to PN19 (Figure 5C). During this timeframe, the proportion of phagocytic microglia with thick processes (≥ 68 %) was higher than the proportion of phagocytic microglia with thin processes (≥ 16 %). By PN17, the proportion of microglia with thick processes decreased ~ 16 % keeping that proportion until PN19. In contrast, the proportion of microglia with thin processes increased ~ 17 % between PN15 and PN17 maintaining a similar proportion of cells until PN19 (Figure 5C).

Phagocytic cups are largest during the third postnatal week in both the GL and ML.

We quantified the size of individual phagocytic cups and a 2 x 4 ANOVA analysis detected a significant main effect of age ($p < 0.000$)[n]. Pairwise comparisons revealed PN17 cerebellums have larger phagocytic cups than those found at PN10 ($p = 0.06$), PN14 ($p < 0.000$) and PN21 ($p = 0.003$) (Figure 5D). There was no impact of cerebellar layer on cup size ($p = 0.09$)[o].

Pyknotic bodies are more prevalent in the GL than the ML only during the first postnatal week.

We quantified the density of pyknotic bodies in the cerebellar cortex (Figure 6B) at different postnatal time points in order to establish a pattern of cell death and to see if it correlated with the pattern of increased phagocytosis at PN17. A significant interaction between age X cerebellar layer for pyknotic bodies was detected ($p < 0.000$)[p]. Pyknotic bodies density decreased in the GL at PN14 ($p < 0.000$), PN17 ($p < 0.000$) and PN21 ($p < 0.000$) compared to PN7, but not at PN5 ($p = 0.751$) (Figure 6A). No changes in the density of pyknotic bodies were detected in the ML in any of the developmental time points analyzed when compared to PN7 (PN5; $p = 0.199$, PN14; $p = 0.688$, PN17; $p = 0.487$, PN21; $p = 0.375$; Figure 6). Moreover, there were more pyknotic bodies in the GL than the ML at PN5 ($p < 0.000$) and PN7 ($p < 0.000$), but not at later ages (PN14; $p = 0.134$, PN17; $p = 0.922$, PN21; $p = 0.194$; Figure 6A). These data indicate there is not a clear relationship between the appearance of both phagocytic cups and pyknotic bodies in the developing cerebellum.

We also found co-localization of pyknotic cell bodies within some phagocytic cups in the cerebellar cortex at PN17 (Figure 6C). As expected, the cell death marker cleaved caspase-3 also co-localized with some phagocytic cups at PN17 (Figure 6D). However, we also detected cleaved caspase-3 broadly in the cerebellar cortex and white matter, with an intense expression in the Purkinje cell layer. This did not appear related to cell cel death (see discussion below).

Males have more microglia with thin processes than females in the GL at PN17.

We looked at sex differences in the cerebellum in terms of microglia density at PN17 in both the GL and ML in order to determine whether at this unique time point the cerebellum develops differently according to sex. We found that males have a higher density of microglia with thin processes than females in the GL ($p = 0.026^{t}$; Figure 7D). No significant differences were found in any other of the morphological categorization of microglia in the GL (round/amoeboid; $t_{(4)} = 0.000^{q}$, stout; $p = 0.270^{r}$, with thick processes; $p = 0.127^{s}$, Figure 7A-C) or the ML (round/amoeboid; $p = 0.375^{u}$, stout; $p = 0.646^{v}$, with thick processes; $p = 0.168^{w}$, with thin processes; $p = 0.137^{x}$, Figure 7E-H). Also, there were no significant differences between males and females for phagocytic cups in the GL ($p = 0.356)^{y}$ or ML ($p = 0.159)^{z}$. The same results were found for total microglia (GL; $p = 0.423^{aa}$, ML; $p = 0.256^{bb}$).

Discussion

The rat cerebellum reaches maturation during the first three postnatal weeks and undergoes remarkable anatomical changes during this time (Heinsen, 1977; Altman, 1982; Goldowitz and Hamre, 1998; Sotelo, 2004; Sillitoe and Joyner, 2007; Butts et al., 2014). We found microglia also dramatically change their morphological profile from round to ramified in the cerebellar cortex during this dynamic period of development (Figure 1B). This developmental profile of microglia in the cerebellum is consistent with previous findings in other regions of the CNS, i.e., going from round to ramified morphology (Wu et al., 1992; Schwarz et al., 2012). However, morphological differences in microglia varied by subregion (ML versus GL), suggesting an important role for local factors in regulating differentiation. A decline in round/amoeboid microglia after the first postnatal week in the entire mouse cerebellum has also been reported, although with a different developmental profile (Ashwell, 1990). The frequency of stout microglia also declined along a similar time course to the amoeboid, whereas microglia with both thick and thin processes increased as the cerebellum matured. These data indicate a continuous process of microglial maturation during the first three postnatal weeks that might be related

376 to a specific function as the cerebellum develops including regulation of cell death and synaptic
377 pruning.

378 Microglia remove apoptotic cellular debris through phagocytosis (Parnaik et al., 2000;
379 Neumann et al., 2009; Sierra et al., 2010; Sierra et al., 2013). Phagocytosis by ramified microglia (with
380 thick or thin processes) requires the formation of round structures of actin called 'phagocytic cups'
381 (Swanson, 2008). The appearance of a marked increase in phagocytic cups during the third postnatal
382 week, particularly at PN17, suggests this is a critical period for microglial phagocytosis in the
383 developing cerebellum. Moreover, the content of some phagocytic cups indicated pyknotic bodies,
384 suggesting the engulfment of apoptotic cells, as has been observed in other regions of the CNS (Sierra
385 et al., 2010). Previous evidence of microglial phagocytosis in the developing cerebellum focused on
386 round or amoeboid microglia (Ashwell, 1990). Here we show that ramified microglia are the dominant
387 committers of phagocytosis during the second and third postnatal week of development in the
388 cerebellum. However, how phagocytic microglia contribute to the establishment of the cerebellar
389 circuit remains poorly understood.

390 The cerebellar cortex is organized into three anatomical layers that contain different types of
391 neurons with specific developmental timeframes and populations (Altman, 1982; Sotelo, 2004). The
392 GL consists of a larger variety and population of cells compared to the ML and the Purkinje layer that
393 only contains two different interneurons and one type of neuron, respectively (Burgoyne and Cambray-
394 Deakin, 1988; Voogd and Glickstein, 1998; Apps and Garwicz, 2005). We observed differences
395 between the GL and ML in terms of microglial population. The overall number of microglia are
396 consistently higher in the GL than the ML from PN12 to PN21, but interestingly, this pattern changes
397 when the morphology of microglia is taken into account. While more stout microglia are present in the
398 ML than the GL during the second and third postnatal week, there are more microglia with thin
399 processes in the GL than the ML, but only during the third postnatal week. Stout microglia are still

differentiating and changing into the ramified form as part of their maturation likely in their final location in the cerebellar cortex. On the other hand, microglia with thin processes have already reached their final location in the cerebellar cortex increasing in cell density as the cerebellum matures. Thus, our findings indicate that microglia are not uniformly distributed in the cerebellar cortex of the developing cerebellum, a finding consistent with a previous report in the young (>25 days) and adult mouse cerebellum (>90 days) (Vela et al., 1995).

A surprising observation was the high degree of regional and temporal specificity of the phagocytic activity of microglia, an important function for the normal developing brain as well as in the adult brain under infectious or damage situations (Neumann et al., 2009; Sierra et al., 2013). Phagocytosis by microglia was higher in the ML during the second postnatal week but a few days later the GL had dramatically more phagocytic cups until the end of the third week. This switch may be driven by a combination of processes occurring in the GL required for its maturation such as cell proliferation and formation of synapses (Altman, 1972; Burgoyne and Cambray-Deakin, 1988; Carletti and Rossi, 2008), but also cell death.

We found a peak of phagocytic cups density at PN17 which was localized to the GL and which persisted for a three-day window in the third postnatal week of development. During this window the proportion of microglia with thick processes decreased ~ 16 % while the proportion of microglia with thin processes increased ~ 17 %, suggesting a final maturation phase. Although this change is related to maturation of the cerebellum, whether it is critical for the establishment of the GL remains unknown. We found no evidence to suggest the increased phagocytosis at PN17 was solely for the removal of dead cells since the pattern of pyknotic bodies, a measure of cell death, bore no resemblance to the pattern of microglial phagocytosis. Similar results in the mouse developing cerebellum are in accordance with ours (Wood et al., 1993; Lossi et al., 2002). Nonetheless, the co-localization of pyknotic bodies and cleaved caspase-3 with some phagocytic cups at PN17 in the cerebellar cortex,

indicates microglia are removing apoptotic cells. Interestingly, our observation of cleaved caspase-3 expression broadly in the cerebellum suggests it may be participating in non-apoptotic processes such as cell differentiation, cell proliferation, neurite pruning and synaptic plasticity as described by others (Oomman et al., 2004; D'Amelio et al., 2012; Hyman and Yuan, 2012; Shalini et al., 2015). The removal of apoptotic cells by ramified microglia is supported by the size of the phagocytic cups, which correlates with the size of granule neurons (Burgoyne and Cambray-Deakin, 1988), the only neurons proliferating during the second and third postnatal weeks in the cerebellum (Carletti and Rossi, 2008). Nevertheless, synaptic and axonal debris could also undergo removal by microglia as part of the synaptic changes and maturation of the climbing and mossy fibers at this age (Goldowitz and Hamre, 1998; Hashimoto and Kano, 2005; McKay and Turner, 2005).

Microglia regulate synapses and axons during development in other regions of the CNS during the second and third postnatal weeks (Berbel and Innocenti, 1988; Tremblay et al., 2010; Paolicelli et al., 2011; Schafer et al., 2012). This implicates microglia as being directly involved in the remodeling of neural synaptic circuits. By the second postnatal week rat pups generally open their eyes (Reiter et al., 1975) and also begin to respond to auditory signals (Friauf, 1992). By the third postnatal week play behavior appears (Meaney and Stewart, 1981; Panksepp, 1981; Auger and Olesen, 2009).Thus, the cerebellum processes motor and sensorial stimulation that may regulate synaptic connections and therefore, the phagocytic activity of microglia.

We measured the size of phagocytic cups and found them to differ according to age, but not to location in the cerebellar cortex. The size of the cups was largest on PN17, when phagocytosis peaks in the GL, but not in the ML. This finding suggests phagocytic microglia are engulfing either larger or greater amounts of cellular debris at PN17. The difference between the largest and the smallest phagocytic cup was equal to 1 μm, which might indicate a precise and efficient process of phagocytic cup formation. However, whether this difference carries a significant biological function is not clear.

448 Evidence in this study supports the conclusion that PN17 is an important time point for
449 microglia function in the development of the cerebellum. This function depends on the location of
450 microglia in the cerebellar cortex, but we also found sex to influence microglia in the cerebellum as
451 males showed more microglia with thin processes than females in the GL, but not in the ML, at PN17.
452 Microglia with thin processes presumably have reached their final location in the cerebellar cortex; and
453 therefore, they are matured and surveying their local environment suggesting a different pattern in
454 microglial maturation in the GL according to sex that might influence the assembly of the cerebellar
455 circuit. However, there was no sex difference in frequency of phagocytic cups in the cerebellar layers at
456 this age, indicating that phagocytosis by microglia is similar between males and females in the
457 developing cerebellum. Sex differences have been reported in both the adult human and rat cerebellums
458 in terms of anatomy and function (Dean and McCarthy, 2008). Here we show a sex difference at the
459 cellular level in a structure vulnerable to damage during development. The cerebellum is commonly
460 altered in developmental disorders such as autism, a disorder with gender bias in its prevalence
461 (Bauman and Kemper, 2005; Amaral et al., 2008; Perez-Pouchoulen et al., 2012; Werling and
462 Geschwind, 2013). Therefore, these results might give insights to address other ways to explore the
463 developing cerebellum under normal and abnormal conditions.

464 Altogether, this work contributes to the understanding of the role of microglia in the rat
465 cerebellum during normal development with a particular focus on the development of the vermis, a
466 vulnerable structure to developmental alterations. To understand what is inadequate in the abnormal
467 developing cerebellum we have to understand first how the cerebellum is formed and the contribution
468 of microglia to this end.

469

470

471 **References**

472

473 Abraham H, Tornoczky T, Kosztolanyi G, Seress L (2001) Cell formation in the cortical layers of the
474 developing human cerebellum. Int J Dev Neurosci 19:53-62.

475 Altman J (1972) Postnatal development of the cerebellar cortex in the rat. II. Phases in the maturation
476 of Purkinje cells and of the molecular layer. J Comp Neurol 145:399-463.

477 Altman J (1982) Morphological Development of the Rat Cerebellum and Some of Its Mechanism. Exp
478 Brain Res Suppl. 6:8-49.

479 Amaral DG, Schumann CM, Nordahl CW (2008) Neuroanatomy of autism. Trends Neurosci 31:137-
480 145.

481 Apps R, Garwicz M (2005) Anatomical and physiological foundations of cerebellar information
482 processing. Nat Rev Neurosci 6:297-311.

483 Apps R, Hawkes R (2009) Cerebellar cortical organization: a one-map hypothesis. Nat Rev Neurosci
484 10:670-681.

485 Ashwell K (1990) Microglia and cell death in the developing mouse cerebellum. Dev Brain Res
486 55:219-230.

487 Auger AP, Olesen KM (2009) Brain sex differences and the organisation of juvenile social play
488 behaviour. J Neuroendocrinol 21:519-525.

489 Ayoub AE, Salm AK (2003) Increased morphological diversity of microglia in the activated
490 hypothalamic supraoptic nucleus. J Neurosci 23:7759-7766.

491 Bauman ML, Kemper TL (2005) Neuroanatomic observations of the brain in autism: a review and
492 future directions. Int J Dev Neurosci 23:183-187.

493 Berbel P, Innocenti GM (1988) The development of the corpus callosum in cats: a light- and electron-
494 microscopic study. J Comp Neurol 276:132-156.

495 Burgoyne RD, Cambray-Deakin MA (1988) The cellular neurobiology of neuronal development: the
496 cerebellar granule cell. Brain Res 472:77-101.

497 Butts T, Green MJ, Wingate RJ (2014) Development of the cerebellum: simple steps to make a 'little
498 brain'. Development 141:4031-4041.

499 Carletti B, Rossi F (2008) Neurogenesis in the cerebellum. Neuroscientist 14:91-100.

500 Catalin B, Cupido A, Iancau M, Albu CV, Kirchhoff F (2013) Microglia: first responders in the central
501 nervous system. Rom J Morphol Embryol 54:467-472.

502 Cuadros MA, Rodriguez-Ruiz J, Calvente R, Almendros A, Marin-Teva JL, Navascues J (1997)
503 Microglia development in the quail cerebellum. J Comp Neurol 389:390-401.

504 D'Amelio M, Sheng M, Cecconi F (2012) Caspase-3 in the central nervous system: beyond apoptosis.
505 Trends Neurosci 35:700-709.

506 Dean SL, McCarthy MM (2008) Steroids, sex and the cerebellar cortex: implications for human
507 disease. Cerebellum 7:38-47.

508 Durisko C, Fiez JA (2010) Functional activation in the cerebellum during working memory and simple
509 speech tasks. Cortex 46:896-906.

510 Friauf E (1992) Tonotopic Order in the Adult and Developing Auditory System of the Rat as Shown by
511 c-fos Immunocytochemistry. Eur J Neurosci 4:798-812.

512 Glickstein M (1992) The cerebellum and motor learning. Curr Opin Neurobiol 2:802-806.

513 Glickstein M, Strata P, Voogd J (2009) Cerebellum: history. Neuroscience 162:549-559.

514 Goldowitz D, Hamre K (1998) The cells and molecules that make a cerebellum. Trends Neurosci
515 21:375-382.

516 Gomez-Gonzalez B, Escobar A (2010) Prenatal stress alters microglial development and distribution in
517 postnatal rat brain. Acta Neuropathol 119:303-315.

518 Gottwald B, Mihajlovic Z, Wilde B, Mehdorn HM (2003) Does the cerebellum contribute to specific
519 aspects of attention? Neuropsychologia 41:1452-1460.

520 Haraguchi S, Sasahara K, Shikimi H, Honda S, Harada N, Tsutsui K (2012) Estradiol promotes
521 purkinje dendritic growth, spinogenesis, and synaptogenesis during neonatal life by inducing
522 the expression of BDNF. Cerebellum 11:416-417.

523 Hashimoto K, Kano M (2005) Postnatal development and synapse elimination of climbing fiber to
524 Purkinje cell projection in the cerebellum. Neurosci Res 53:221-228.

525 Heinsen H (1977) Quantitative anatomical studies on the postnatal development of the cerebellum of
526 the albino rat. Anat Embryol (Berl) 151:201-218.

527 Holstege G, Georgiadis JR, Paans AM, Meiners LC, van der Graaf FH, Reinders AA (2003) Brain
528 activation during human male ejaculation. J Neurosci 23:9185-9193.

529 Hyman BT, Yuan J (2012) Apoptotic and non-apoptotic roles of caspases in neuronal physiology and
530 pathophysiology. Nat Rev Neurosci 13:395-406.

531 Ito D, Imai Y, Ohsawa K, Nakajima K, Fukuuchi Y, Kohsaka S (1998) Microglia-specific localisation
532 of a novel calcium binding protein, Iba1. Brain Res Mol Brain Res 57:1-9.

533 Kaur C, Sivakumar V, Zou Z, Ling EA (2014) Microglia-derived proinflammatory cytokines tumor
534 necrosis factor-alpha and interleukin-1beta induce Purkinje neuronal apoptosis via their
535 receptors in hypoxic neonatal rat brain. Brain Struct Funct 219:151-170.

536 Lenz KM, Nugent BM, Haliyur R, McCarthy MM (2013) Microglia are essential to masculinization of
537 brain and behavior. J Neurosci 33:2761-2772.

538 Lossi L, Mioletti S, Merighi A (2002) Synapse-independent and synapse-dependent apoptosis of
539 cerebellar granule cells in postnatal rabbits occur at two subsequent but partly overlapping
540 developmental stages. Neuroscience 112:509-523.

541 Marin-Teva JL, Dusart I, Colin C, Gervais A, van Rooijen N, Mallat M (2004) Microglia promote the
542 death of developing Purkinje cells. Neuron 41:535-547.

543 McKay BE, Turner RW (2005) Physiological and morphological development of the rat cerebellar
544 Purkinje cell. J Physiol 567:829-850.

545 Meaney M, Stewart J (1981) A descriptive study of social development in the rat (rattus norvegicus).
546 Anim Behav 29:34-45.

547 Miquel M, Toledo R, Garcia LI, Coria-Avila GA, Manzo J (2009) Why should we keep the cerebellum
548 in mind when thinking about addiction? Curr Drug Abuse Rev 2:26-40.

549 Moulton EA, Schmahmann JD, Becerra L, Borsook D (2010) The cerebellum and pain: passive
550 integrator or active participator? Brain Res Rev 65:14-27.

551 Moulton EA, Elman I, Becerra LR, Goldstein RZ, Borsook D (2014) The cerebellum and addiction:
552 insights gained from neuroimaging research. Addict Biol 19:317-331.

553 Murdoch BE (2010) The cerebellum and language: historical perspective and review. Cortex 46:858-
554 868.

555 Nayak D, Roth TL, McGavern DB (2014) Microglia development and function. Annu Rev Immunol
556 32:367-402.

557 Neumann H, Kotter MR, Franklin RJ (2009) Debris clearance by microglia: an essential link between
558 degeneration and regeneration. Brain 132:288-295.

559 Nimmerjahn A, Kirchhoff F, Helmchen F (2005) Resting microglial cells are highly dynamic
560 surveillants of brain parenchyma in vivo. Science 308:1314-1318.

561 Oomman S, Finckbone V, Dertien J, Attridge J, Henne W, Medina M, Mansouri B, Singh H,
562 Strahlendorf H, Strahlendorf J (2004) Active caspase-3 expression during postnatal
563 development of rat cerebellum is not systematically or consistently associated with apoptosis. J
564 Comp Neurol 476:154-173.

565 Panksepp J (1981) The ontogeny of play in rats. Dev Psychobiol 14:327-332.

566 Paolicelli RC, Bolasco G, Pagani F, Maggi L, Scianni M, Panzanelli P, Giustetto M, Ferreira TA,
567 Guiducci E, Dumas L, Ragozzino D, Gross CT (2011) Synaptic pruning by microglia is
568 necessary for normal brain development. Science 333:1456-1458.

569 Parnaik R, Raff MC, Scholes J (2000) Differences between the clearance of apoptotic cells by
570 professional and non-professional phagocytes. Curr Biol 10:857-860.

571 Perez-Pouchoulen M, Miquel M, Saft P, Brug B, Toledo R, Hernandez ME, Manzo J (2012) The
572 cerebellum in Autism. e-neurobiologia 3:1-11.

573 Ransohoff RM, Perry VH (2009) Microglial physiology: unique stimuli, specialized responses. Annu
574 Rev Immunol 27:119-145.

575 Rapoport M, van Reekum R, Mayberg H (2000) The role of the cerebellum in cognition and behavior:
576 a selective review. J Neuropsychiatry Clin Neurosci 12:193-198.

577 Reiter LW, Anderson GE, Laskey JW, Cahill DF (1975) Developmental and behavioral changes in the
578 rat during chronic exposure to lead. Environ Health Perspect 12:119-123.

579 Saab CY, Willis WD (2003) The cerebellum: organization, functions and its role in nociception. Brain
580 Res Brain Res Rev 42:85-95.

581 Sarna JR, Hawkes R (2003) Patterned Purkinje cell death in the cerebellum. Prog Neurobiol 70:473-
582 507.

583 Schafer DP, Lehrman EK, Kautzman AG, Koyama R, Mardinly AR, Yamasaki R, Ransohoff RM,
584 Greenberg ME, Barres BA, Stevens B (2012) Microglia sculpt postnatal neural circuits in an
585 activity and complement-dependent manner. Neuron 74:691-705.

586 Schwarz JM, Sholar PW, Bilbo SD (2012) Sex differences in microglial colonization of the developing
587 rat brain. J Neurochem 120:948-963.

588 Shalini S, Dorstyn L, Dawar S, Kumar S (2015) Old, new and emerging functions of caspases. Cell
589 Death Differ 22:526-539.

590 Sierra A, Abiega O, Shahraz A, Neumann H (2013) Janus-faced microglia: beneficial and detrimental
591 consequences of microglial phagocytosis. Front Cell Neurosci 7:6.

592 Sierra A, Encinas JM, Deudero JJ, Chancey JH, Enikolopov G, Overstreet-Wadiche LS, Tsirka SE,
593 Maletic-Savatic M (2010) Microglia shape adult hippocampal neurogenesis through apoptosis-
594 coupled phagocytosis. Cell Stem Cell 7:483-495.

595 Sillitoe RV, Joyner AL (2007) Morphology, molecular codes, and circuitry produce the three-
596 dimensional complexity of the cerebellum. Annu Rev Cell Dev Biol 23:549-577.

597 Sotelo C (2004) Cellular and genetic regulation of the development of the cerebellar system. Prog
598 Neurobiol 72:295-339.

599 Strata P (2015) The Emotional Cerebellum. Cerebellum

600 Strick PL, Dum RP, Fiez JA (2009) Cerebellum and nonmotor function. Annu Rev Neurosci 32:413-
601 434.

602 Swanson JA (2008) Shaping cups into phagosomes and macropinosomes. Nat Rev Mol Cell Biol
603 9:639-649.

604 Tanaka M (2009) Dendrite formation of cerebellar Purkinje cells. Neurochem Res 34:2078-2088.

605 ten Donkelaar HJ, Lammens M, Wesseling P, Thijssen HO, Renier WO (2003) Development and
606 developmental disorders of the human cerebellum. J Neurol 250:1025-1036.

607 Tremblay ME, Lowery RL, Majewska AK (2010) Microglial interactions with synapses are modulated
608 by visual experience. PLoS Biol 8:e1000527.

609 Tremblay ME, Stevens B, Sierra A, Wake H, Bessis A, Nimmerjahn A (2011) The role of microglia in
610 the healthy brain. J Neurosci 31:16064-16069.

611 Vargas DL, Nascimbene C, Krishnan C, Zimmerman AW, Pardo CA (2005) Neuroglial activation and
612 neuroinflammation in the brain of patients with autism. Ann Neurol 57:67-81.

613 Vela JM, Dalmau I, Gonzalez B, Castellano B (1995) Morphology and distribution of microglial cells
614 in the young and adult mouse cerebellum. J Comp Neurol 361:602-616.

615 Voogd J, Glickstein M (1998) The anatomy of the cerebellum. Trends Neurosci 21:370-375.

616 Werling DM, Geschwind DH (2013) Sex differences in autism spectrum disorders. Curr Opin Neurol
617 26:146-153.

618 Williamson LL, Sholar PW, Mistry RS, Smith SH, Bilbo SD (2011) Microglia and memory:
619 modulation by early-life infection. J Neurosci 31:15511-15521.

620 Wood KA, Dipasquale B, Youle RJ (1993) In situ labeling of granule cells for apoptosis-associated
621 DNA fragmentation reveals different mechanisms of cell loss in developing cerebellum. Neuron
622 11:621-632.

623 Wu CH, Wen CY, Shieh JY, Ling EA (1992) A quantitative and morphometric study of the
624 transformation of amoeboid microglia into ramified microglia in the developing corpus
625 callosum in rats. J Anat 181 (Pt 3):423-430.

626

627

628

629

630 **Figure Legends**

631 **Figure 1. Postnatal microglia across the developing cerebellum.** (A) A sagittal view of the vermis
632 showing the six lobules used to count microglia (blue background). (B) The density of total microglia
633 significantly increased by 1.58-fold in the third postnatal week compared to the first week (*$p < 0.05$,
634 **$p \leq 0.01$ when compared to PN5; data are expressed as mean ± S.E.M.; n = 4, 2 males + 2 females
635 for each group). Colored bars depict the proportion of microglia according to morphology at different
636 time points during postnatal development: round/amoeboid microglia are present but infrequent during
637 the first ten postnatal days while stout microglia are strongly predominant during the first postnatal
638 week, and microglia with both thick and thin processes are more abundant during the second and third
639 week, respectively. PN = postnatal day.
640
641 **Figure 2. Morphological profile of microglia in the postnatal developing cerebellum.** (A) The
642 frequency of round/amoeboid microglia significantly decreased after the first postnatal week (B) as
643 well as stout microglia. (C) Conversely, the density of microglia with thick processes increased only
644 during the second postnatal week followed by a decrease in the third postnatal week. (D) The density of
645 microglia with thin processes gradually increased after the first postnatal week doubling their density
646 by the third postnatal week. (E) Sagittal views of the mid-vermis, labeled with Iba1, across the first
647 three postnatal weeks. All data are expressed as mean ± S.E.M. (n = 4, 2 males + 2 females for each
648 group). Significant differences are detonated by *$p < 0.05$, **$p < 0.01$, ***$p < 0.000$ compared to PN5.
649 Inserts depict a higher magnification of selected microglia (red squares) in each panel. Scale bars = 100
650 µm (gray scale images), insert's scale bars = 25 µm (color images), and panel E scale bars = 500 µm
651 (from PN5 to PN21). Images in panel A, B, C and D depict the morphology of microglia at two
652 different postnatal ages: PN7 (A and B) and PN12 (C and D). PN = postnatal day.
653

Figure 3. Microglial phagocytosis in the postnatal developing cerebellum. (A) The highest density of phagocytic cups was observed during the third postnatal week at PN17 (***$p < 0.000$ compared to PN5, PN7, PN10, PN12, PN14 and PN21; n =4, 2 males + 2 females for each group). Data are expressed as mean ± S.E.M. (B) Phagocytic cups exhibited by microglia (red arrows) in the developing cerebellum at PN17 (scale bar = 100 µm). (C) Microglia with phagocytic cups (top) or microglia without phagocytic cups (bottom row) at different time points during postnatal development (scale bars = 25 µm). PN = postnatal day.

Figure 4. Microglia location in the cerebellar cortex based on morphological classification. (A) Total microglia were significantly higher in the GL than the ML during the second and third postnatal week in the cerebellum (*$p < 0.05$, **$p < 0.01$, ***$p < 0.000$). (B) The density of round/amoeboid microglia was very low and did not differ between the ML and the GL from PN12 to PN21. (C) The density of stout microglia was significantly higher in the ML than the GL at all days examined except PN14 (**$p < 0.01$, ***$p < 0.000$). (D) Microglia with thick processes were the most abundant but did not differ between the ML and the GL. (E) There were significantly more microglia with thin processes in the GL than the ML at PN17 and PN21 but not at younger ages examined (*$p < 0.05$, ***$p < 0.000$). All data are expressed as mean ± S.E.M. (n = 6, 3 males + 3 females for each group). PN = postnatal day.

Figure 5. Frequency of phagocytosis by microglia changes by location in the cerebellar cortex across development. (A) The density of phagocytic cups was higher in the ML than the GL at PN12 (**$p < 0.01$), and PN14 (*$p < 0.05$), but switched at PN17 (***$p < 0.000$) and PN21 (*$p < 0.05$), so that the GL exhibited more phagocytic cups than the ML. The highest density of phagocytic cups was found in the GL at PN17 compared to PN12, PN14 and PN21 ($^{@}p < 0.000$). Scale bar = 100 µm. (B) Proportion of microglia that exhibited phagocytic cups in the GL at PN17: 67 % of all phagocytic

679 microglia had thick processes and 33 % had thin processes. No round/amoeboid or stout microglia
680 showed phagocytic cups. (C) A difference in the density of phagocytic cups was found at younger ages
681 (PN15; $^{**}p = 0.003$, and PN16; $^{*}p = 0.05$) compared to PN17, but no significant differences were
682 found at older ages (PN18; $p = 0.583$, and PN19; $p = 0.615$). In contrast, in the ML, the density of
683 phagocytic cups was lower only at PN19 ($^{\wedge}p = 0.043$) compared to PN17. Additionally, a difference in
684 the density of phagocytic cups between the GL and ML was found from PN16 to PN19 (PN16; $^{\#}p <$
685 0.000, PN17; $^{+}p < 0.000$, PN18; $^{\&}p < 0.000$, and PN19; $^{@}p < 0.000$) but not at PN15 ($p = 0.467$) (n = 6,
686 3 males + 3 females for each group for panel A, B and C). In this experiment the density of phagocytic
687 cups was not counted in animals at PN21 but the dashed lines depict the pattern previously observed at
688 the end of the third postnatal week in both the GL and ML (Figure 5A). (D) The diameter of microglial
689 phagocytic cups was bigger on PN17 compared to PN10 ($^{@}p = 0.06$, see effect size estimation in table
690 **2**), PN14 ($^{*}p < 0.000$) and PN21 ($^{\#}p = 0.003$). All data are expressed as mean ± S.E.M. (^n = 4, 2 males
691 + 2 females; *n = 8, 4 males + 4 females: ^PN10, *PN14, *PN17 and *PN21). PN = postnatal day; GL
692 = granular layer; ML = molecular layer.
693
694 **Figure 6. Identification of pyknotic bodies by Nissl staining in the postnatal developing**
695 **cerebellum.** (A) The density of pyknotic bodies (red arrows) decreased only in the GL after the first
696 postnatal week at PN14, PN17 and PN21 ($^{***}p < 0.000$), but not at PN7 ($p = 0.302$), compared to PN5.
697 No changes in the density of pyknotic bodies were detected in the ML across the developmental time
698 points analyzed when compared to PN7 (PN5; $p = 0.199$, PN14; $p = 0.688$, PN17; $p = 0.487$, PN21; $p =$
699 0.375). The GL exhibited more pyknotic bodies than the ML only during the first postnatal week at
700 PN5 ($^{\#}p < 0.000$) and PN7 ($^{\wedge}p < 0.000$). Scale bar = 25 µm. Data are expressed as mean ± S.E.M. (*n =
701 6, 3 males + 3 females; ^n = 4, 2 males + 2 females: *PN5, ^PN7, *PN14, *PN17 and *PN21). (B)
702 PN7 cerebellar sagittal section stained with cresyl violet showing pyknotic bodies pointed out by red
703 arrows (ML = molecular layer, GL = granular layer, PkL = Purkinje layer, EGL = external granular

layer). **(C)** Confocal co-localization of a pyknotic body (fragmented nucleus in yellow) and a phagocytic cup (red) in the cerebellar cortex at PN17 (scale bars = 15 μm). (D) 3D confocal image depicting a co-localization of a microglial phagocytic cup (red) and a cleaved caspase-3 positive cell (green) at the tip of a microglia process (white arrow). PN = postnatal day.

Figure 7. Microglial sex differences in the developing cerebellum. (A, B, C, D,) Estimated density of microglia based on morphology in the GL at PN17. Males had more microglia with thin processes than females (*$p = 0.026$). No significant differences were found for sex in round/amoeboid microglia, stout microglia ($p = 0.270$) or microglia with thick processes ($p = 0.127$). (E, F, G, H) Estimated density of microglia based on morphology in the ML at PN17. The statistical analysis indicated no sex differences in round/amoeboid ($p = 0.375$), stout ($p = 0.646$), microglia with thick processes ($p = 0.168$) or microglia with thin processes ($p = 0.137$). Data are expressed as mean ± S.E.M. (n = 6, 3 males + 3 females for each group). PN = postnatal day; GL = granular layer; ML = molecular layer.

Table Legends

Table 1. Summary of statistical analysis. Superscript letters in the Result section correspond to rows in the table.

Table 2. Summary of pair comparison tests. Superscript letters in the table correspond to rows in the Results section.

A

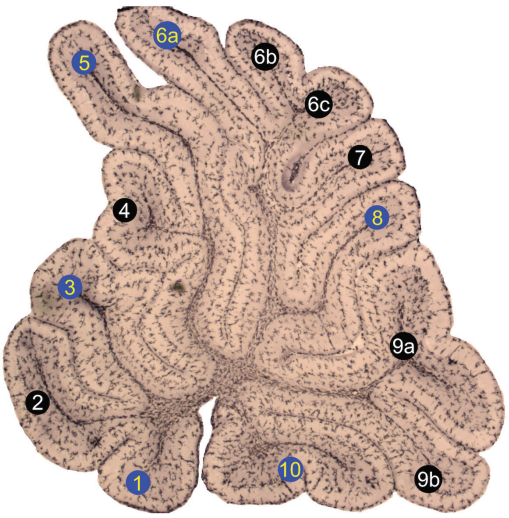

cerebellar lobules

B

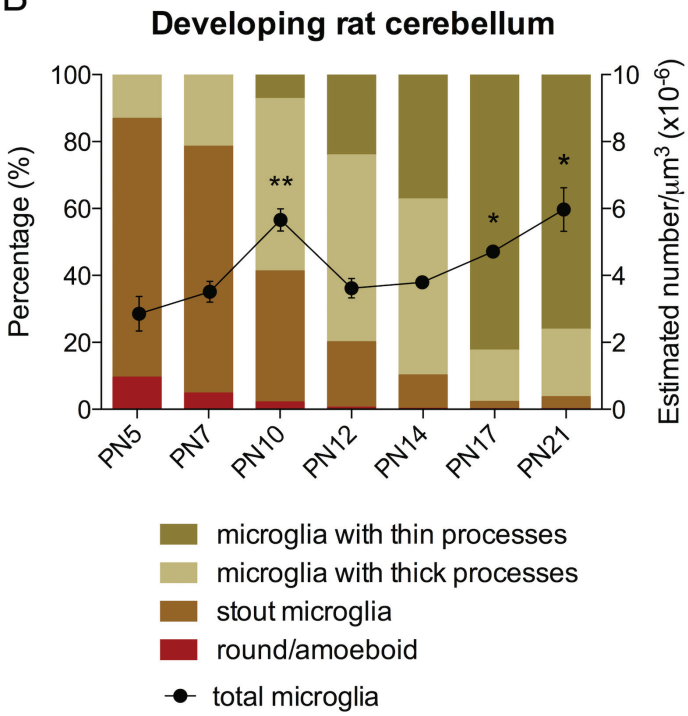

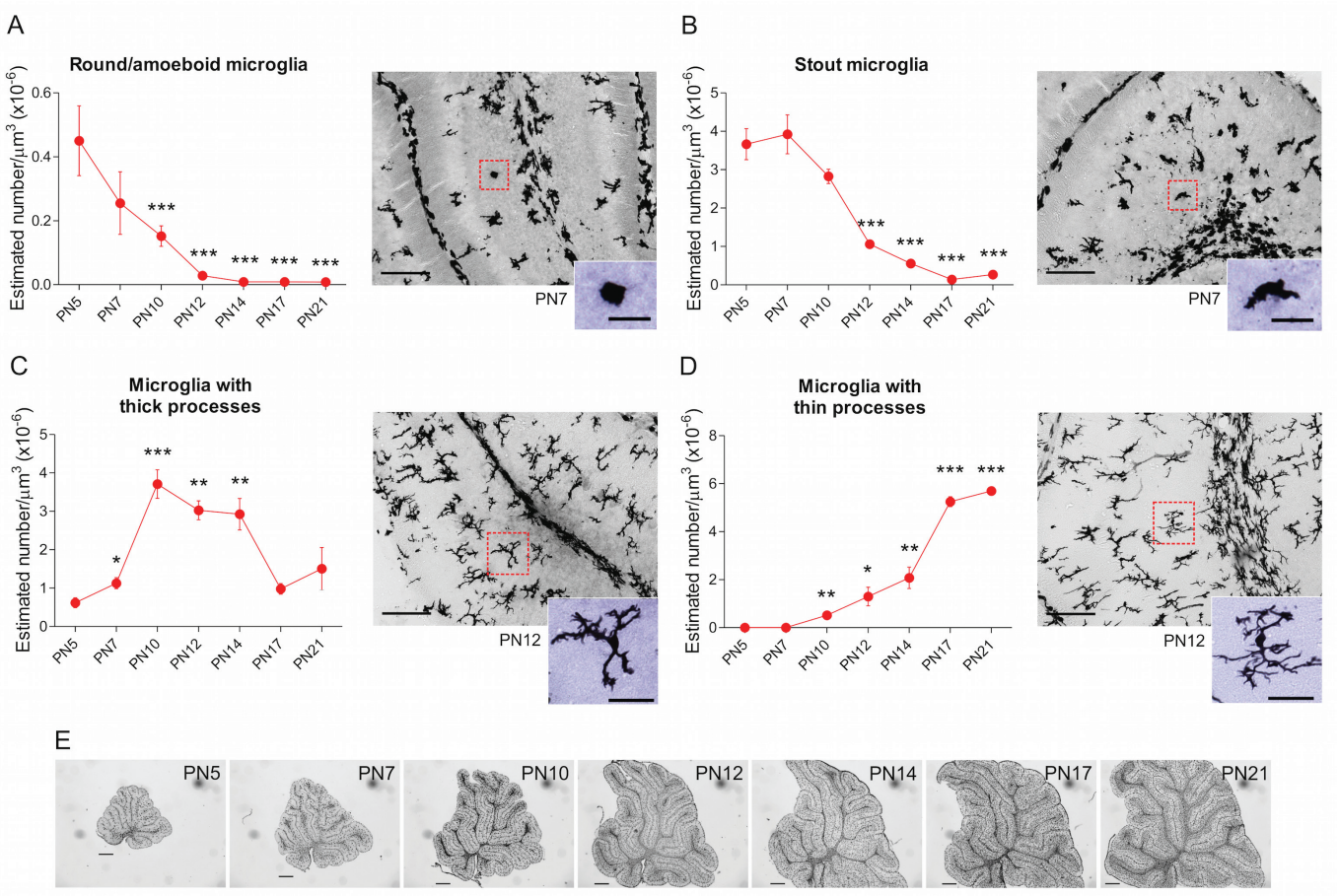

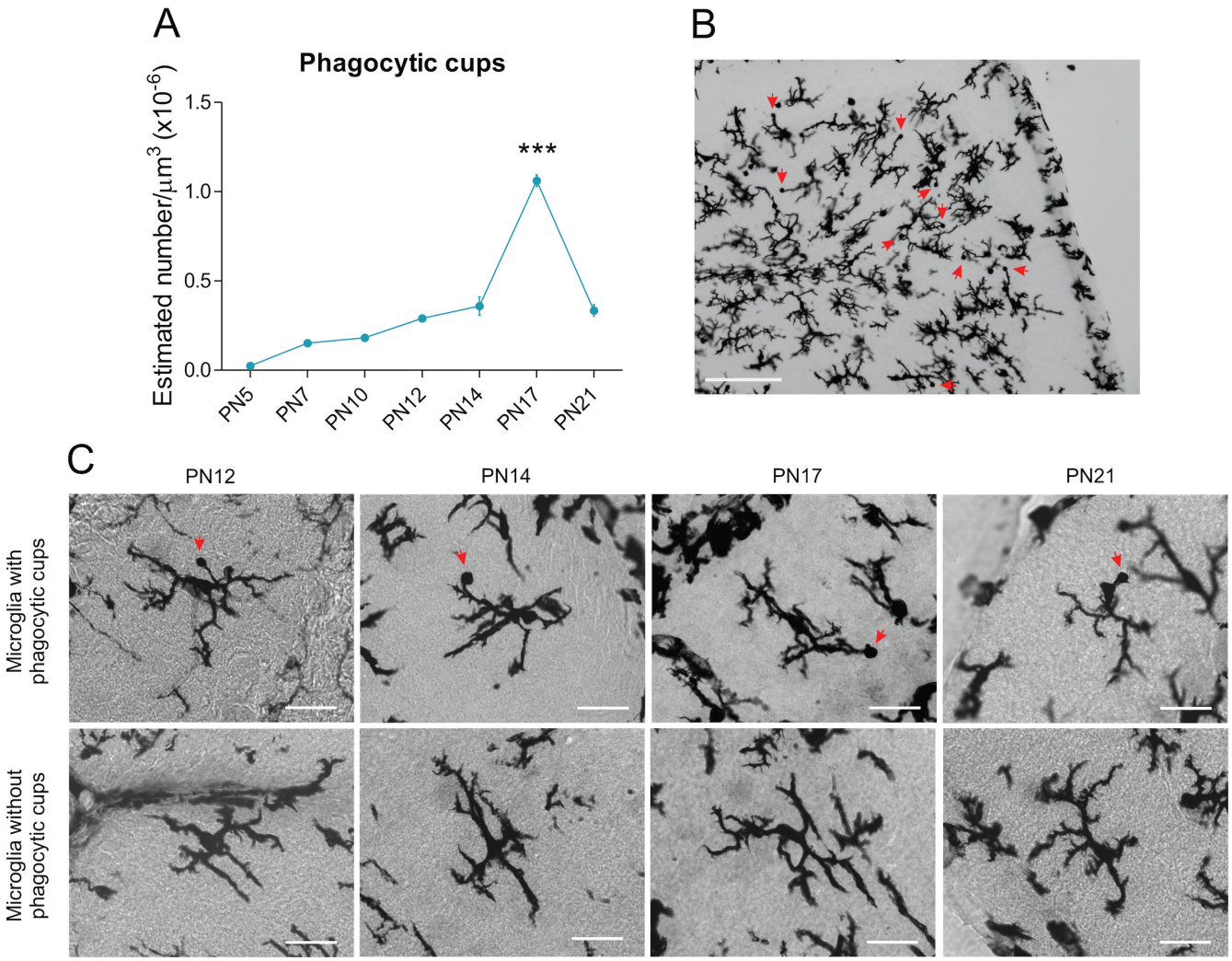

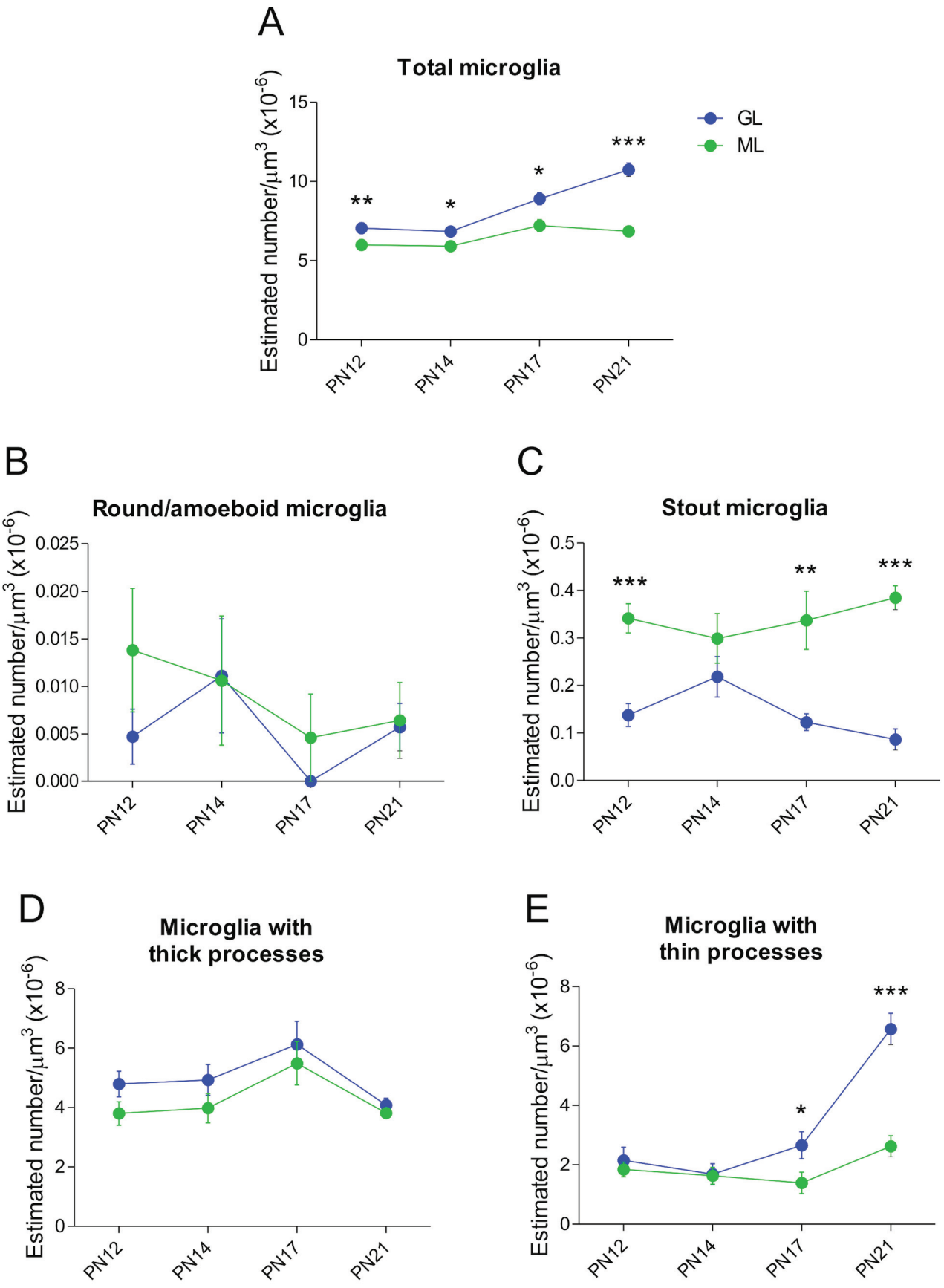

A

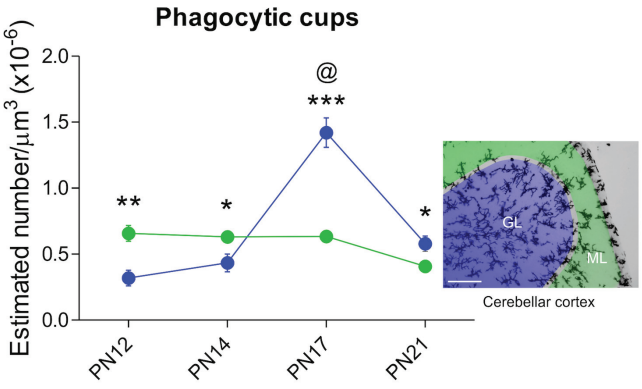

B

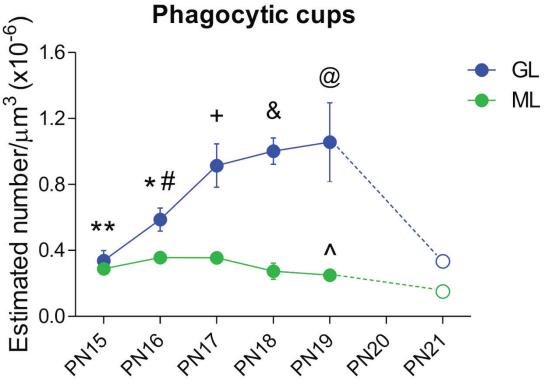

C

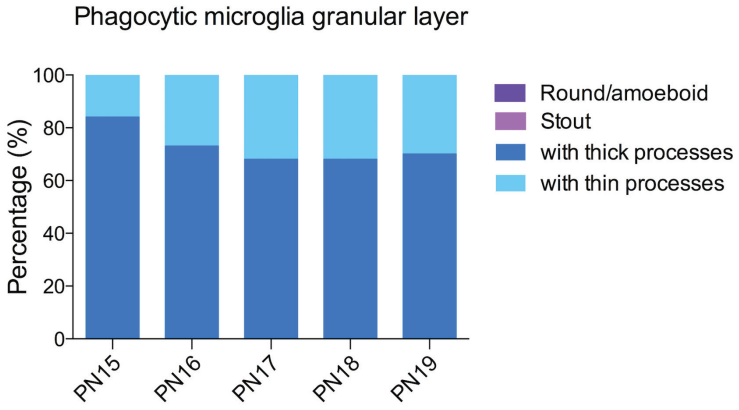

D

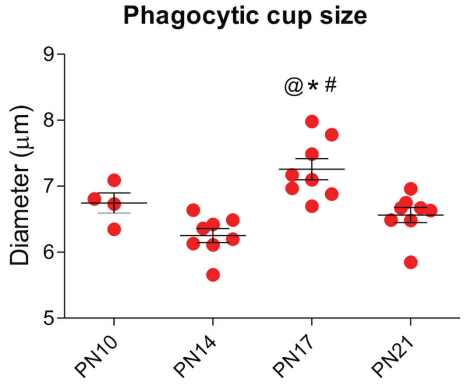

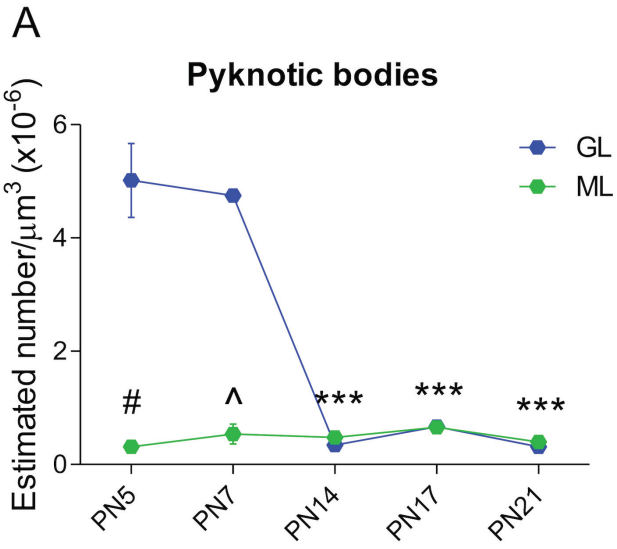

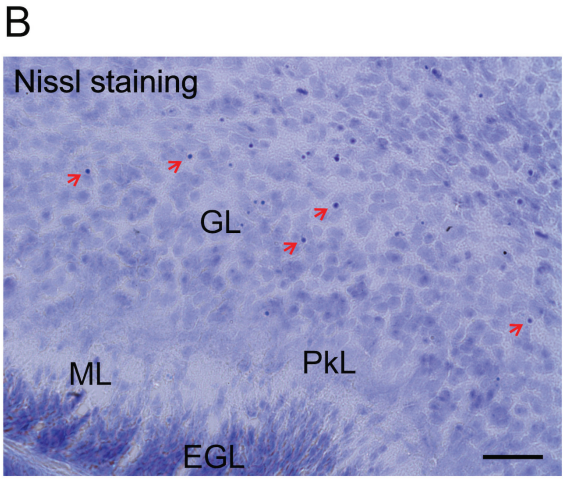

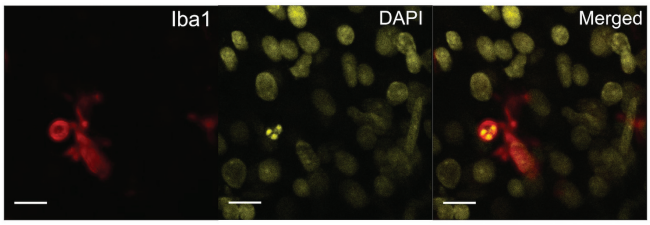

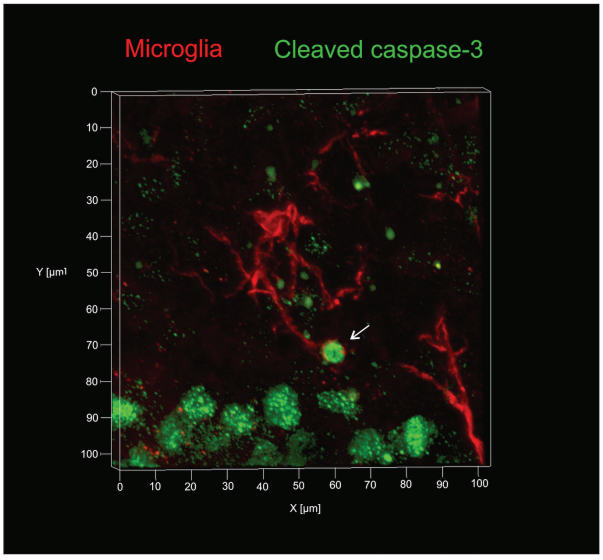

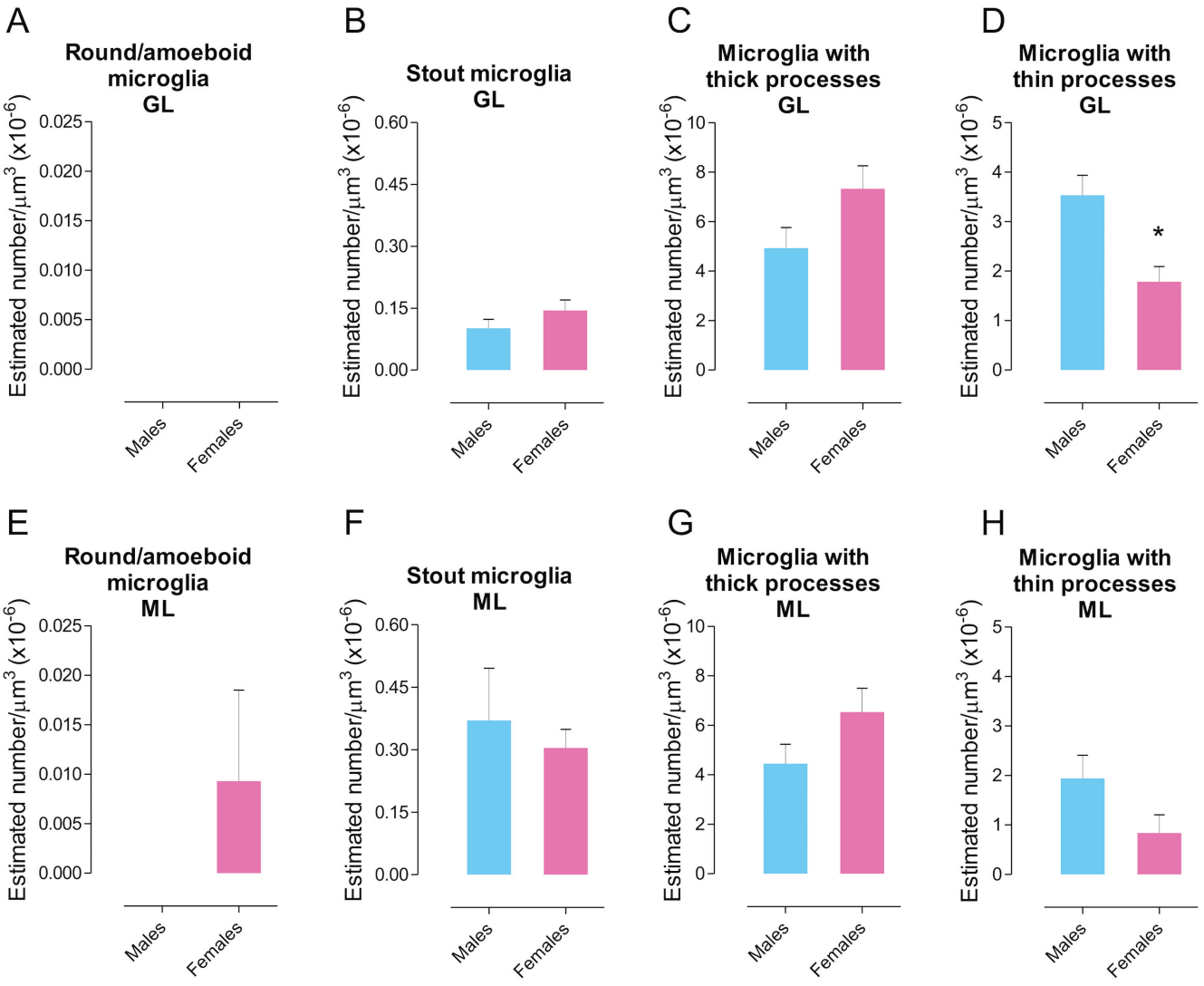

Table 1. Statistical table					
	Data structure	Type of test	Test value	Effect size	Power
a	Normally distributed	One-way ANOVA	$F_{(6, 21)} = 9.559$	$\eta = 0.73$	0.73
b	Normally distributed	One-way ANOVA	$F_{(6, 21)} = 8.895$	$\eta = 0.72$	0.99
c	Normally distributed	One-way ANOVA	$F_{(6, 21)} = 41.022$	$\eta = 0.92$	1.00
d	Normally distributed	One-way ANOVA	$F_{(6, 21)} = 14.074$	$\eta = 0.80$	1.00
e	Normally distributed	One-way ANOVA	$F_{(6, 21)} = 93.160$	$\eta = 0.96$	1.00
f	Normally distributed	One-way ANOVA	$F_{(6, 21)} = 136.664$	$\eta = 0.97$	1.00
g	Normally distributed	Two-way ANOVA	$F_{(3, 48)} = 9.667$	$\eta = 0.42$	0.99
h	Normally distributed	Two-way ANOVA	$F_{(3, 48)} = 0.418$	- - -	0.13
i	Normally distributed	Two-way ANOVA	$F_{(3, 48)} = 2.84$	$\eta = 0.18$	0.64
j	Normally distributed	Two-way ANOVA	$F_{(3, 48)} = 0.221$	- - -	0.09
k	Normally distributed	Two-way ANOVA	$F_{(3, 48)} = 10.517$	$\eta = 0.44$	0.99
l	Normally distributed	Two-way ANOVA	$F_{(3, 48)} = 30.770$	$\eta = 0.69$	1.00
m	Normally distributed	Two-way ANOVA	$F_{(3, 48)} = 5.521$	$\eta = 0.31$	0.97
n	Normally distributed	Two-way ANOVA	$F_{(3, 48)} = 18.271$	$\eta = 0.53$	1.00
o	Normally distributed	Two-way ANOVA	$F_{(3, 48)} = 2.860$	- - -	0.38
p	Normally distributed	Two-way ANOVA	$F_{(3, 48)} = 54.600$	$\eta = 0.83$	1.00
q	- - -	- - -	- -	- - -	- - -
r	t-distribution	Student's t-test	$t_{(4)} = 1.278$	- - -	0.17
s	t-distribution	Student's t-test	$t_{(4)} = 1.920$	- - -	0.48
t	t-distribution	Student's t-test	$t_{(4)} = 3.445$	$d = 3.445$	0.73
u	t-distribution	Student's t-test	$t_{(4)} = 1.000$	- - -	0.12
v	t-distribution	Student's t-test	$t_{(4)} = 0.496$	- - -	0.1
w	t-distribution	Student's t-test	$t_{(4)} = 1.683$	- - -	0.26
x	t-distribution	Student's t-test	$t_{(4)} = 1.858$	- - -	0.30
y	t-distribution	Student's t-test	$t_{(4)} = 1.044$	- - -	0.13
z	t-distribution	Student's t-test	$t_{(4)} = 1.726$	- - -	0.27
aa	t-distribution	Student's t-test	$t_{(4)} = 0.892$	- - -	0.11
bb	t-distribution	Student's t-test	$t_{(4)} = 1.323$	- - -	0.18

Table 2. Pairwise comparisons report.								
Developmental profile of microglia and phagocytic cups.								
			PN7	PN10	PN12	PN14	PN17	PN21
a	Total microglia	compared to PN5	$t_{(6)} = 4.534$	$t_{(6)} = 4.534$ $d = 3.70$	$t_{(6)} = 1.277$	$t_{(6)} = 1.782$	$t_{(6)} = 4.534$ $d = 3.70$	$t_{(6)} = 4.534$ $d = 3.70$
b	Amoeboid microglia	compared to PN5	$t_{(6)} = 1.330$	$t_{(6)} = 2.621$ $d = 2.14$	$t_{(6)} = 3.845$ $d = 3.13$	$t_{(6)} = 4.045$ $d = 3.30$	$t_{(6)} = 4.043$ $d = 3.30$	$t_{(6)} = 4.044$ $d = 3.30$
c	Stout microglia	compared to PN5	$t_{(6)} = 0.395$	$t_{(6)} = 1.886$	$t_{(6)} = 6.416$ $d = 5.23$	$t_{(6)} = 7.634$ $d = 6.23$	$t_{(6)} = 8.654$ $d = 7.06$	$t_{(6)} = 8.373$ $d = 6.83$
d	Microglia with thick processes	compared to PN5	$t_{(6)} = 2.659$ $d = 2.17$	$t_{(6)} = 7.858$ $d = 6.41$	$t_{(6)} = 8.657$ $d = 7.06$	$t_{(6)} = 5.344$ $d = 4.36$	$t_{(6)} = 1.926$	$t_{(6)} = 1.574$
e	Microglia with thin processes	compared to PN5	$t_{(6)} = 1.000$	$t_{(6)} = 5.078$ $d = 4.14$	$t_{(6)} = 3.352$ $d = 2.73$	$t_{(6)} = 4.653$ $d = 3.79$	$t_{(6)} = 25.466$ $d = 20.79$	$t_{(6)} = 31.079$ $d = 25.37$
f	Phagocytic cup	compared to PN17	PN5 $t_{(6)} = 29.336$ $d = 23.95$	PN7 $t_{(6)} = 26.068$ $d = 21.28$	PN10 $t_{(6)} = 24.687$ $d = 20.15$	PN12 $t_{(6)} = 20.255$ $d = 16.53$	PN14 $t_{(6)} = 11.571$ $d = 9.44$	PN21 $t_{(6)} = 15.762$ $d = 12.86$
Microglia and phagocytic cups in the ML and GL during postnatal development.								
g	Total microglia	compared to ML	GL $t_{(10)} = 3.356$ $d = 2.12$	GL $t_{(10)} = 2.640$ $d = 1.66$	GL $t_{(10)} = 3.160$ $d = 1.99$	GL $t_{(10)} = 7.438$ $d = 4.70$		
h	Amoeboid microglia	compared to ML	GL $t_{(10)} = 1.226$	GL $t_{(10)} = 0.049$	GL $t_{(10)} = 1.000$	GL $t_{(10)} = 0.139$		
i	Stout microglia	compared to ML	GL $t_{(10)} = 5.209$ $d = 3.29$	GL $t_{(10)} = 1.192$	GL $t_{(10)} = 3.354$ $d = 2.12$	GL $t_{(10)} = 8.846$ $d = 5.59$		
j	Microglia with thick processes	compared to ML	GL $t_{(10)} = 1.703$	GL $t_{(10)} = 1.326$	GL $t_{(10)} = 0.601$	GL $t_{(10)} = 1.003$		
k	Microglia with thin processes	compared to ML	GL $t_{(10)} = 0.604$	GL $t_{(10)} = 0.116$	GL $t_{(10)} = 2.191$ $d = 1.38$	GL $t_{(10)} = 6.186$ $d = 3.91$		
l	Phagocytic cup	compared to ML	GL $t_{(10)} = 4.013$ $d = 2.53$	GL $t_{(10)} = 2.400$ $d = 1.51$	GL $t_{(10)} = 6.814$ $d = 4.30$	GL $t_{(10)} = 2.279$ $d = 1.44$		

Table 2. Pairwise comparisons report (continuation).								
Microglial phagocytic activity during the third postnatal week of development.								
			PN15	PN16	PN18	PN19		
m	Phagocytic cup	compared to GL PN17	GL $t_{(10)} = 3.978$ $d = 2.51$	GL $t_{(10)} = 2.198$ $d = 1.39$	GL $t_{(10)} = 0.568$	GL $t_{(10)} = 0.518$		
m	Phagocytic cup	compared to ML PN17	ML $t_{(10)} = 1.499$	ML $t_{(10)} = 0.029$	ML $t_{(10)} = 1.300$	ML $t_{(10)} = 2.313$ $d = 1.46$		
			PN15	PN16	PN17	PN18	PN19	
m	Phagocytic cup	compared to the ML	GL $t_{(10)} = 0.757$	GL $t_{(10)} = 3.052$ $d = 1.93$	GL $t_{(10)} = 4.091$ $d = 2.58$	GL $t_{(10)} = 7.765$ $d = 4.91$	GL $t_{(10)} = 3.348$ $d = 2.11$	
Phagocytic cup size during the third postnatal week of development.								
			PN10	PN14	PN21			
n	Phagocytic cup	compared to PN17	$t_{(10)} = 2.037$ $d = 1.28$	$t_{(14)} = 5.262$ $d = 2.81$	$t_{(14)} = 3.547$ $d = 1.73$			
Pyknotic bodies in the GL than the ML during postnatal development.								
			PN5	PN14	PN17	PN21		
p	Pyknotic bodies	compared to GL PN7	GL $t_{(8)} = 0.328$	GL $t_{(8)} = 34.179$ $d = 24.16$	GL $t_{(8)} = 25.394$ $d = 17.95$	GL $t_{(8)} = 39.642$ $d = 28.03$		
p	Pyknotic bodies	compared to ML PN7	ML $t_{(8)} = 1.401$	ML $t_{(8)} = 0.416$	ML $t_{(8)} = 0.729$	ML $t_{(8)} = 0.939$		
			PN5	PN7	PN14	PN17	PN21	
p	Pyknotic bodies	compared to ML	GL $t_{(10)} = 7.163$ $d = 4.53$	GL $t_{(6)} = 19.461$ $d = 15.88$	GL $t_{(10)} = 1.628$	GL $t_{(10)} = 0.100$	GL $t_{(10)} = 1.392$	

Table 2. Pairwise comparisons report (continuation).								
Sex differences in microglia morphology on PN17 cerebellum.								
			GL	ML				
q / u	Amoeboid microglia	compared to females	males $t_{(4)} = 0.000$	males $t_{(4)} = 1.000$				
r / v	Stout microglia	compared to females	males $t_{(4)} = 1.278$	males $t_{(4)} = 0.496$				
s / w	Microglia with thick processes	compared to females	males $t_{(4)} = 1.920$	males $t_{(4)} = 1.683$				
t / x	Microglia with thin processes	compared to females	males $t_{(4)} = 3.445$ $d = 3.445$	males $t_{(4)} = 1.858$				
y / z	Phagocytic cup	compared to females	males $t_{(4)} = 1.044$	males $t_{(4)} = 1.726$				
aa / bb	Total microglia	compared to females	males $t_{(4)} = 0.892$	males $t_{(4)} = 1.323$				